Skin Protective Effects of Acid-stress Sorghum Fermentation by Extremophile *Monascus pilosus* against UV-induced Inflammation and Photoaging

Yuxi Zheng,[a,b,†] Han Luo,[b,†] Nianhui Ding,[c] Yan Huang,[d] Kai Wang,[e] Chun Li,[f] Chaolong Zhang,[f] and Jianguo Feng [c,*]

Ultraviolet (UV) radiation causes skin damage including oxidative stress, inflammation, and photoaging. Extremophile fermentation products have been found to effectively protect the skin from UV-induced damage. This study aimed to investigate the impact of acid-induced stress on the content of bioactive compounds, as well as the anti-inflammatory and anti-photoaging properties of sorghum fermentation by the extremophilic *Monascus pilosus*. The study compared acid-stress fermentation (ASF) of sorghum with conventional fermentation (CF) and examined differences in total phenolic content, antioxidant activity, and short-chain fatty acid levels. Using gas chromatography–mass spectrometry assay, the ASF sample had lower total phenolic content compared to CF, but significantly higher levels of short-chain fatty acids. Butyric acid was the predominant metabolite in the ASF sample, followed by propionic acid. The ASF sample exhibited superior protection for UV-irradiated human keratinocytes by inhibiting apoptosis, reducing ROS, and downregulating inflammatory mediators. It also decreased metalloproteinases expression levels, increased collagen and elastin production, and mitigated UV-induced photoaging. The effects of ASF samples were evaluated in volunteers, and the results confirmed the ASF sample's effectiveness in ameliorating UV-induced skin symptoms, including pigmentation, redness, and wrinkles. These findings conclude that acid-stress enhances the anti-inflammatory and anti-photoaging capabilities of *Monascus pilosus* fermented sorghum.

DOI: 10.15376/biores.19.3.5239-5261

Keywords: Acid stress; Extremophile; Fermentation; Inflammation; Monascus pilosus; Photoaging

Contact information: a: Moutai Institute, Renhuai 564500*, Guizhou Province, China; b: Kweichow Moutai Distillery Co., Ltd., Renhuai, Guizhou Province,* 564500 *China; c: Anesthesiology and Critical Care Medicine Key Laboratory of Luzhou, The Affiliated Hospital, Southwest Medical University, Luzhou, Sichuan Province,* 646000 *China; d: Department of Dermatology, Suining First People's Hospital, Suining, Sichuan,* 629000 *China; e: Technology Centre of China Tobacco Yunnan Industrial Co., Ltd., Kunming, Yunnan Province,* 650231 *China; f: Chengdu Baolu Biotechnology Co., Ltd., Chengdu, Sichuan Province,* 610000 *China. †These authors contributed equally; *Corresponding author: fengjianguo@swmu.edu.cn*

INTRODUCTION

The skin undergoes a gradual and irreversible aging process. Unlike internal organs, the skin is directly exposed to the external environment, making it susceptible to the effects of sunlight. Studies have shown that photoaging, primarily induced by sun ultraviolet (UV) radiation is the primary external factor contributing to skin aging, responsible for over 80% of facial aging (Fitsiou *et al*. 2021). The most notable histological differences between

photoaged and naturally aged skin are the excessive accumulation of amorphous elastic fibers in the dermis of photoaged skin and the significant abnormalities in the breakage and structure of collagen fibers. Excessive UV exposure disrupts the integrity of the skin barrier and significantly decreases its secretory function. This, in turn, significantly elevates the risk of skin inflammation and the development of cutaneous malignancies (Rittie and Fisher 2015; Schuch *et al*. 2017). Therefore, it is imperative to impede photoaging and protect the skin barrier to prevent and treat skin-related diseases. These efforts not only hold significant academic value but also offer notable practical applications.

Oxidative stress (OS) plays a pivotal role in the skin photoaging progression (Gu *et al*. 2020). Upon exposure of the skin to UV irradiation, intracellular chromophores such as nicotinamide adenine dinucleotide/nicotinamide adenine dinucleotide phosphate, tryptophan, and riboflavin absorb light energy. In the presence of molecular oxygen, these chromophores become activated, leading to the generation of several oxidation products, such as reactive oxygen species (ROS), encompassing superoxide anions, hydroxyl radicals, and O_2-derived non-radicals (*e.g.*, H_2O_2). With prolonged exposure to UV irradiation, the escalating intracellular ROS levels disrupt intracellular redox homeostasis, resulting in two distinct outcomes: (1) Elevated ROS levels disrupt cellular structure and function, releasing various inflammatory mediators, such as members of the interleukin (IL) family. This process leads to local skin inflammation and further damage. (2) ROS mediate the activation of the receptor tyrosine kinase signaling cascade, initiating several apoptosis-associated signaling pathways, such as the mitogen-activated protein kinase (MAPK) pathway. Consequently, this accelerates the photoaging process by decreasing collagen production and increasing matrix metalloproteinase (MMP) synthesis (Liu *et al*. 2022; Olsen *et al*. 2022).

Extremophiles have evolved unique cellular structures, response mechanisms, and metabolic systems *via* natural selection to cope with elevated OS levels induced by intense stressors (Kruger *et al*. 2018). From a biotechnological standpoint, the plasticity of metabolism and gene expression in extremophiles holds great promise due to their ability to thrive in adverse environments and produce efficient and diverse metabolites under specific conditions (Chen and Jiang 2018). The potential of extremophile fermentation products in mitigating OS induced by environmental stressors has garnered substantial global research attention. However, current research primarily focuses on environmental issues (Huang *et al*. 2019), with no documented literature addressing the utilization of extremophile fermentation products in skincare for countering external environmental stressors.

Moutai-flavored liquor (MFL) has emerged as the preeminent alcoholic beverage in China, occupying an indispensable role within Chinese culture and daily life owing to its unique flavor and exceptional quality (Dai *et al*. 2020). It is extensively manufactured in Moutai Town, Guizhou Province, China. The unique stressed fermentation process employed in the production of MFL entails the cultivation of local brewing microorganisms within a microecological brewing environment characterized by elevated levels of salinity, acidity, and alcohol content. This process encompasses various unique extremophiles, which contribute to the distinctive flavor of MFL. Sorghum, recognized as one of the foremost cereal crops cultivated worldwide, particularly in arid and semi-arid regions, is extensively utilized in food and beverage applications through fermentation processes (Galati *et al*. 2014; Adebo 2020). In addition, it has widely been reported that the sorghum fermentation products derived from these extremophiles contain several bioactive compounds, such as organic acids, polyphenols, flavonoids, amino acids,

triterpenes, and vitamins (Wang *et al*. 2019; Peng *et al*. 2021). The bioactive compounds in sorghum fermentation products can significantly influence the fragrance of distilled spirits (Weiss *et al.* 2022) and they also contribute to making sorghum beer a nutritious beverage, particularly in Africa (Tanwar *et al*. 2023). These compounds also find widespread application in the fields of pharmaceuticals, cosmetics, dietary supplements, and various other health-related products (Sun *et al*. 2020; Osman *et al*. 2022).

In a previous study, an extremophilic filamentous fungal strain, YX-1125, was isolated from the microbial resources of the MFL brewing environment (Zheng *et al*. 2021). This strain was identified as *Monascus pilosus* through both fungal morphology and DNA analysis. Remarkably, through the adjustment of fermentation pH to mimic the extreme conditions found in the MEL brewing environment, this strain demonstrated the highest reported yield of short-chain fatty acids (SCFAs) in the literature (Zheng *et al*. 2021). Several articles have confirmed and corroborated the health benefits associated with microbial SCFAs, including the alleviation of inflammation and the selective inhibition of harmful microorganisms (Lloyd-Price *et al*. 2019; Shahab *et al*. 2020). Therefore, in this study, a novel ingredient derived from *M. pilosus* and sorghum fermentation was evaluated for its ability to counteract UV-induced damage, employing a series of *in vitro* and *in vivo* experiments. This study is the first investigation into the effects of acidic stress during the fermentation process on the anti-inflammatory and antiphotoaging potential of extremophile fermentation products.

EXPERIMENTAL

Raw Materials and Chemicals

The raw material utilized was "Hongyingzi", an organic glutinous sorghum (*Sorghum bicolor* (L.) Moench) cultivated in Moutai Town, Renhuai City, Guizhou Province, China. This sorghum served as the primary raw material for the production of MFL in Moutai Town, boasting a total starch content of 83.4%, with amylopectin accounting for 96.3% of this starch composition (Zhou *et al*. 2020). The sorghum was subjected to milling to obtain a powder using a mesh size of 100 and was subsequently stored at 4 °C. The enzyme α-amylase (intermediate-temperature α-amylase from *Bacillus subtilis*, 4000 U/g) and amyloglucosidase (a compound glucoamylase from *Aspergillus niger* and *B. licheniformis*, 100,000 U/mL) were generously provided by Shandong Nongda Biological Products Co., Ltd. These enzymes were used in the liquefaction process to convert starch into glucose. All other chemical reagents employed in this study were of analytical grade and were purchased from Shanghai Aladdin Bio-Chem Technology Co., Ltd (Shanghai, China, www.aladdin-e.com).

Strains and Seed Preparation

As previously described (Zheng *et al*. 2021), the *M. pilosus* YX-1125 strain was obtained from an MFL brewery located in Moutai Town and is presently housed at the China General Microbiological Culture Center (No. CGMCC 21938). The strain YX-1125 was cultured on potato dextrose agar (PDA) for 5 days at 30 °C and subsequently stored in the refrigerator at either 4 °C (for short-term storage) or -20 °C (for long-term storage). Monthly maintenance involved transferring YX-1125 spores to fresh PDA medium to sustain viability. For the preparation of a fresh spore suspension used for inoculation, the PDA medium was washed with sterile saline. Subsequently, the spore suspension was

incorporated into to a sterile seeding medium (50 g/L glucose, 2.5% yeast extract powder). The spore concentration was standardized to 10^6 spores/mL by adding sterile saline. The seeding suspension of YX-1125 was maintained at 30 °C without aeration, stirring, or shaking for 8 h before its utilization as an inoculum in subsequent fermentation processes.

Lactobacillus plantarum (No. KN-819) was sourced from the Department of Resource Environment at the Moutai Institute. The strain was isolated from the MFL brewery located in Moutai Town. Owing to its notable capacity for high lactic acid production, this strain was employed in the pre-fermentation process for YX-1125 to replicate an acidic stress environment similar to that encountered in MFL brewing (Fig. 1). Prior to utilization, KN-819 was transferred from a 20% glycerol storage medium to a de Man, Rogosa, and Sharpe medium. For the inoculum preparation, the seeding culture was maintained at 30 °C and 150 rpm on a rotary shaker for 12 h, followed by centrifugation at 14,000 ×*g* for 5 min, and subsequently, a sterile saline rinse.

Production of the Fermentation Sample

Figure 1 illustrates the production process of acid stress fermentation (ASF) sample, consisting of three key stages: liquefaction, acidification, and fermentation. The first stage, liquefaction, involved two steps: pre-mashing and saccharification. Briefly, a mixture of distilled water and sorghum powder, with a solid–to–liquid ratio of 1:10 (w/v), was introduced into a shake flask placed in an 80 °C water bath. Subsequently, α-amylase was incorporated into the mixture to attain a final concentration of 140 U/g, facilitating pre-mashing through agitation on a rotary shaker (Shanzhi, Shanghai, China) at 100 rpm for 2 h. The mixture was then cooled to 60 °C and subjected to saccharification at 140 rpm for 8 h, employing a compounded saccharifying enzyme (40 U/g) to completely liberate fermentable sugars from amylopectin. Thereafter, acidification was performed to establish a highly acidic environment conducive to the ensuing stress fermentation, utilizing the lactic acid-producing strain. Following the cooling of the saccharified mash, a 10% inoculum of the lactic acid-producing strain was introduced and incubated at 42 °C under stringent static conditions until the pH reached 3.5. The liquid phase was then collected, ready for the subsequent fermentation stage.

Finally, the ASF sample was produced through fermentation, as described in previous studies, with minor modifications (Zheng *et al*. 2016, 2017). This phase took place in a modified 5-L bulb column bioreactor (Baoxing, Shanghai, China), equipped with a honeycomb structure comprising 60 matrix units to immobilize the filamentous fungus YX-1125. Following 24 h of immobilized culturing, the seeding medium was substituted with the acidified liquid that had been collected. Incubation continued at 35 °C with an aeration rate of 0.5 V/V·min and a stirring rate of 160 rpm. After 96 h, the fermentation broth was collected and filtered through a 1000 Da nanofiltration membrane to eliminate microorganisms and macromolecular impurities, resulting in the production of the ASF sample. The production processes for conventional fermentation (CF) and acidic environment control (AEC) samples are also shown in Fig. 1.

Chemical Characterization of *Monascus* and Sorghum Fermentation Filtrate (MSFF)

Measurement of metabolites

The produced metabolites were analyzed through gas chromatography-mass spectrometry (GC–MS), following the methodology outlined by Mellinas *et al*. (2022), with some modifications). Briefly, dichloromethane was employed as the solvent for

liquid–liquid extraction to obtain the organic phase. Subsequently, active compounds in the MSFF were identified using an Agilent 7890N gas chromatograph coupled with a 5977B quadrupole mass spectrometer (Agilent Technologies, Palo Alto, CA, USA) operating in electron impact ionization mode (70 eV). A DB-WAX capillary column (30 m × 0.25 mm × 0.25 µm) was utilized. Data analysis was performed using the Agilent MSD ChemStation software. The presence of bioactive substances in the samples was determined by comparing the obtained data with a mass spectrometry database maintained by the National Institute of Standards and Technology.

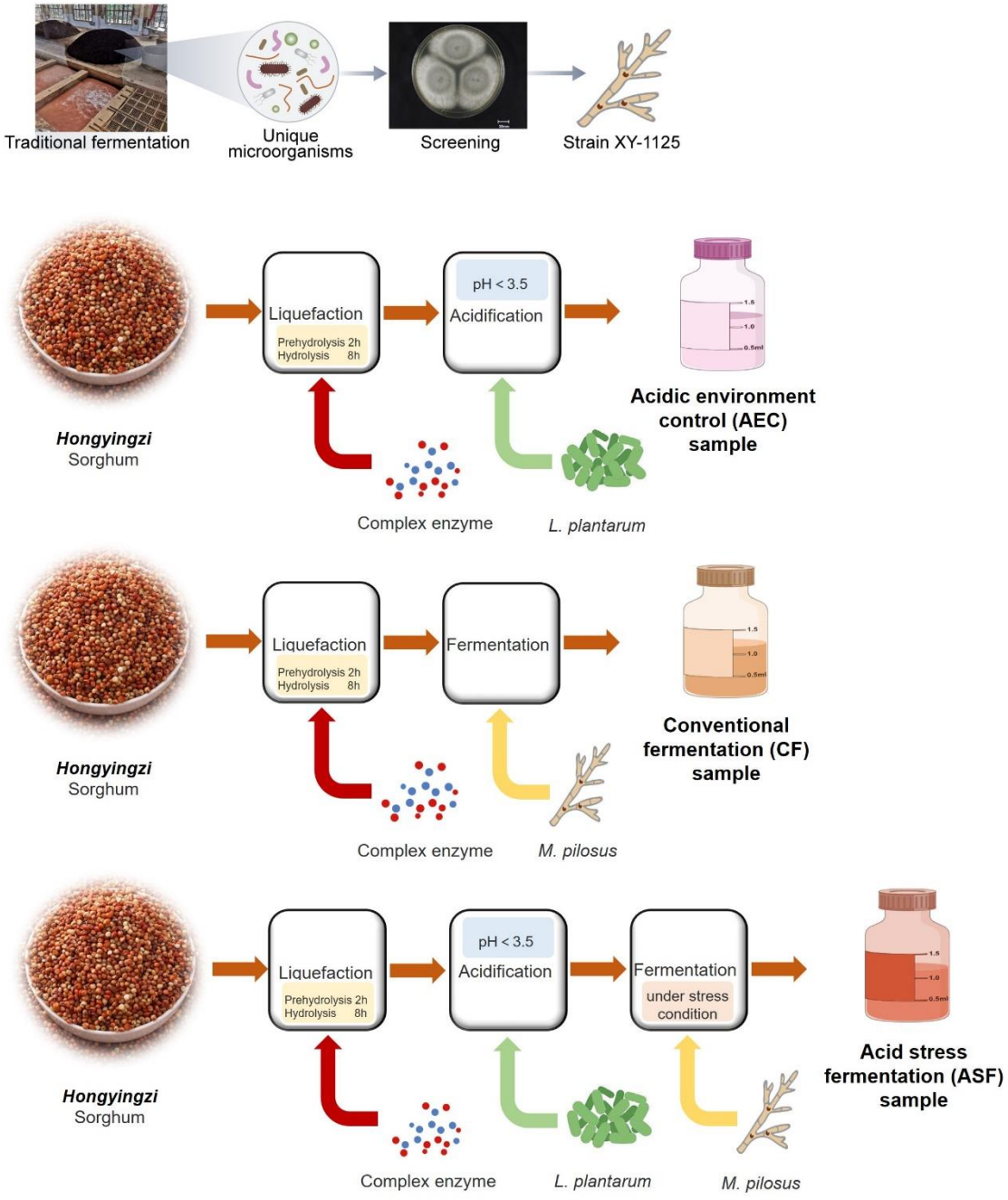

Fig. 1. Schematic illustration of the production process of fermentation samples

Measurement of phenolic compounds

Four major types of phenolic compounds were quantified in the fermentation sample using previously established methods (Dia *et al*. 2016). These included (1) total soluble phenolic acid content, which was determined using a gallic acid standard curve and expressed as milligrams of gallic acid equivalent per milliliter (mg gallic acid eq/mL); (2) total flavonoid content was quantified using a quercetin standard curve and expressed as milligrams of quercetin equivalents per milliliter (mg quercetin eq/mL); (3) total tannin content was assessed through an epicatechin standard curve and expressed as milligrams of epicatechin per milliliter (mg epicatechin eq/mL); and (4) total anthocyanin content was determined spectrophotometrically and expressed as micrograms of glucoside cyanidin-3-glucoside (C3G) per milliliter of the sample (μg cyanidin-3-glucoside eq/mL). All measurements were independently repeated three times.

Antioxidant Activity of the Fermentation Sample

Five criteria were employed to evaluate antioxidant activity, as previously reported (Xu *et al*. 2022): (1) ferrous reducing antioxidant power (FRAP) test, expressed as mmoL eq $FeSO_4$ /mL; (2) 1,1-diphenyl-2-picrylhydrazyl (DPPH) radical scavenging activity; (3) copper and iron chelation abilities; (4) superoxide radical ($O_2^{\bullet -}$) scavenging activity; and (5) hydroxyl radical (HO•) elimination activity.

In vitro Studies

Cell culture and UV irradiation

Human keratinocytes (HaCaT cells, provided by the Stem Cell Bank, Chinese Academy of Sciences) were cultured in Dulbecco's modified Eagle's medium (DMEM) supplemented with 10% fetal bovine serum (FBS) and 1% penicillin/streptomycin at 37 °C with 5% CO_2 and controlled humidity. HaCaT cells were seeded at a density of 7.5×10^4 cells per well in 24-well plates and incubated overnight. Subsequently, they were subjected to a 6-h pretreatment in DMEM containing 0.5% FBS, either with various concentrations of MSFF or sterile distilled water (used as the control). Following pretreatment, the cells were washed twice with phosphate-buffered saline (PBS) to remove any residual DMEM and then covered with a thin layer of PBS before being exposed to 15 mJ/cm^2 of UVB irradiation using a UVB generator (UVP CL-1000 Ultraviolet Crosslinker, Upland, CA, USA).

Cell viability

Cell viability was assessed through sulforhodamine B (SRB) staining (Orellana and Kasinski 2016). Following incubation, cells were rinsed once with sterile PBS and were subsequently fixed in each well with 250 μL of 10% (w/v) trichloroacetic acid, followed by a 1 h-incubation period at 4 °C. Following the rinsing of the plate with slowly flowing tap water, excess water was removed using paper towels, and the plates were air-dried at room temperature (20 to 25 °C). For staining, 250 μL of 0.057% (w/v) SRB solution was applied to each well for 30 min. Unbound dye was removed using 1% (v/v) acetic acid. The protein-bound dye was dissolved in 250 μL of a 10 mM Tris base solution, and 100 μL of the resultant solution was transferred to a 96-well plate for optical density measurement at 510 nm wavelength using a microplate reader.

Measurement of intracellular ROS

Intracellular ROS were quantified using 2′,7′-dichlorodihydrofluorescein diacetate

(DCF-DA). Briefly, HaCaT cells were pretreated with fermentation samples for 6 h prior to UVB irradiation. After 2 h post UVB irradiation, these cells were stained with 5 μM DCF-DA at 37 °C for 30 min, followed by two washes with PBS, and lysed using a solution of 90% dimethyl sulfoxide in PBS. Fluorescence intensity was measured at excitation/emission wavelengths of 485/525 nm using a fluorescent microplate reader.

Enzyme-linked immunosorbent assay (ELISA)

HaCaT cell culture supernatant was collected at 24 h after UVB irradiation. The levels of IL-6 and IL-8 in the culture medium were quantified utilizing an ELISA kit (BioLegend, San Diego, CA, USA) according to the manufacturer's instructions. Subsequently, the absorbance at 450 nm wavelength was measured using a microplate reader.

Western blot

Western blot was employed to detect protein expression levels. The treated cells were harvested, rinsed with PBS, and lysed using RIPA buffer to obtain whole-cell lysates. The resulting supernatant was collected for protein quantification *via* the Bradford protein assay, and a standard curve was established using the bovine serum albumin method (Beyotime, China). Subsequently, cell lysates were separated using sodium dodecyl sulfate–polyacrylamide gel electrophoresis. The proteins in the gel were transferred onto a nitrocellulose membrane. Following blocking with skim milk, the membranes were incubated overnight at 4 °C with primary antibodies against β-actin (Santa Cruz Biotechnology, USA), MMP-1 (Abcam, USA), and MMP-9 (Abcam, USA). Finally, the membranes underwent three washes with tris-buffered saline containing Tween 20 (for 5 min each time) to remove the primary antibodies. Subsequently, the membranes were incubated with corresponding secondary antibodies (Proteintech, China) for 1 h at room temperature. Chemiluminescence detection (BeyoECL Plus, Millipore) was used to visualize the bands of immunoreactive proteins.

In vivo Studies

Four clinical factors were evaluated to examine the *in vivo* effects of fermentation samples, namely facial wrinkles, periorbital wrinkles (PW), melanin levels, and facial redness. This study involved 36 healthy volunteers between the ages of 35 and 65, who were required to spend more than 6 h outdoors daily due to their occupational obligations. Volunteers were excluded from participation if they met any of the following criteria: (1) pregnancy, lactating, or smoking; a history of skin infections, inflammatory acne, or photosensitive dermatoses; or a predisposition to scarring; (2) Prior participation in a study involving topical vitamin A treatment within the 6 months preceding their enrollment in this study. (3) Recent use of systemic retinoids within the past 12 months. (4) Undergoing ablative/non-ablative laser skin resurfacing treatment in the 3 months preceding the study period, and known allergy or sensitivity to weakly acidic solutions. The present study adopted a randomized, double-blind, placebo-controlled trial, design, adhering to the principles outlined in the WMA Declaration of Helsinki (Carlson *et al*. 2004).

All volunteer tests of volunteers adhered to the Cosmetic Safety Technical Specifications (2015, China) and the Practice for the Evaluation of Cosmetic Efficacy Claims, as prescribed by the State Food and Drug Administration of China. The study protocol was approved by the Ethics Committee of BioTruly Cosmetic Dermatology Laboratory and the Institutional Ethics Committee of West China Hospital, Sichuan

University (No. 532, 2022). Informed consent forms were duly signed by all participating volunteers.

In all experiments, researchers assessed clinical safety by assessing topical tolerability, which encompassed factors such as erythema, dryness, flaking, burning sensation, and pruritus, in addition to monitoring any adverse events reported by the participants. These participants read and signed an informed consent form provided by the investigator. One week prior to the start of the study and throughout the study, the participants refrained from using any supplementary skincare, cosmetic, or hygiene products that could potentially influence the study outcomes. During the course of the investigation, researchers followed a regimen of daily facial cleansing for the volunteers, followed by the application of 1 mL/cm^2 of diluted fermentation samples (at a concentration of 5%) or a placebo (distilled water) onto the designated skin testing area. The application process involved gentle massaging until complete absorption of the solution achieved.

Instrumental Evaluations

At the outset (T_0) and at the conclusion (6 weeks later, T_{6w}) of the study, the following instrumental assessments were conducted. Prior to the evaluation, study participants underwent a skin acclimatization period of a minimum of 30 min in a room set to room temperature (22 ± 2 °C) and relative humidity (60% ± 5%). PW, pigmentation, redness, and the texture index (TI) were examined using the Antera3D device (Miravex, Dublin, Ireland), equipped with a camera for capturing and analyzing skin images. The Antera3D system has been widely employed in numerous skin-related studies (Rerknimitr *et al*. 2019; Maitriwong *et al*. 2020). In contrast to conventional imaging methods that rely on a limited set of color channels (red, green, and blue), Antera3D uses reflectance mapping at seven different wavelengths, covering the entire visible spectrum. This allows for more precise observation and analysis of skin redness and pigmentation by measuring hemoglobin and melanin levels. In addition, the device facilitates concurrent assessment of skin texture in different areas.

Statistical Analysis

The data were analyzed with GraphPad Prism software v6.0 (GraphPad Software, San Diego, CA, USA). Parametric analysis of variance test and Tukey's test were used to assess the normality of the sample distribution.

RESULTS

Chemical Characterization of MSFF

Metabolite composition analysis

As shown in Table 1, butyric acid emerged as the predominant metabolite (in both ASF and CF samples constituting over 60% of the total SCFAs), followed by propionic acid. Notably, ASF significantly improved the efficiency of SCFA by *M. pilosus* YX-1125 during fermentation. In contrast, CF redirected metabolic flux towards the production of by-products, particularly ethanol and propanediol. This shift is supported by a five-fold increase in ethanol production, rising from 2.77 g/L to 13.82 g/L. Furthermore, CF exhibited a substantial reduction in both SCFA production and their proportion compared to ASF. Moreover, lactic acid was the primary metabolite in the AEC sample (data not

shown). The results revealed that acid stress can effectively enhance the production of SCFAs by *M. pilosus* YX-1125 when sorghum is used as the substrate.

Table 1. Contents of Metabolites in ASF and CF Samples

Metabolites (g/L)	CF	ASF
Butyric acid	9.76 ± 0.45	15.40 ± 1.04 *
Propionic acid	4.35 ± 0.24	3.23 ± 0.31 *
Lactic acid	N/D	2.54 ± 0.07
Ethanol	13.82 ± 0.79	2.77 ± 0.14 *
Propanol	N/D	3.98 ± 0.15
Propanediol	1.22 ± 0.04	N/D
Butanol	N/D	0.75 ± 0.14

N/D: not detected.* Denotes significant differences between the same metabolite ($p < 0.05$).

Analysis of phenolic contents

Spectroscopic analysis was employed to quantify the phenolic content in three distinct samples, as detailed in Table 2. The results revealed that the phenolic concentrations varied among the different fermentation samples. In the ASF sample, the total tannin exhibited the highest concentration (3.59 mg epicatechin eq/mL) among all total phenolics, consistent with prior findings (Shen *et al*. 2018; Zhou *et al*. 2020) that "Hongyingzi" sorghum possesses a high tannin content. Phenolic acids constituted the second most abundant phenolic compounds at 1.52 mg gallic acid eq/mL. In contrast, the AEC sample contained higher concentrations of all phenolic compounds than the other samples, with the exception of total tannin. Additionally, there was a reduction in phenolic acids in both ASF and CF samples after fermentation with *M. pilosus* YX-1125, suggesting a potential capacity for phenolic degradation by *M. pilosus* YX-1125. In conclusion, the fermentation process negatively impacted phenolic contents, resulting in lower levels in ASF samples compared to CF and AEC.

Table 2. Phenolic Contents in AEC, CF, and ASF Samples as Measured by Spectroscopy

Items	Units	AEC	CF	ASF
PAs	mg gallic acid eq/mL	1.79 ± 0.02 [a]	0.85 ± 0.04 [c]	1.52 ± 0.05 [b]
TFs	mg quercetin eq/mL	0.51 ± 0.02 [a]	0.48 ± 0.03 [a]	0.49 ± 0.01 [a]
TTs	mg epicatechin eq/mL	5.13 ± 0.86 [b]	7.12 ± 0.64 [a]	3.59 ± 0.55 [c]
TDs	μg luteolinidin eq/mL	9.16 ± 0.45 [a]	8.98 ± 0.54 [a]	8.36 ± 0.91[a]
TAs	μg cyanidin-3-glucoside eq/mL	19.43 ± 0.81[a]	16.04 ± 0.40 [b]	13.40 ± 0.38 [c]

TDs: Total 3-deoxyanthocyanidins; TAs: Total Anthocyanins; TFs: Total Flavonoids; PAs: Phenolic acids; TTs: Total Tannins. Different small letters within the same item are significantly different ($p < 0.05$).

Antioxidant Activity of Fermentation Samples

Multiple assays were employed to evaluate the *in vitro* antioxidant potential of fermentation samples, with the results presented in Table 3. The generation of hydroxyl radicals, a common type of ROS induced by UV irradiation, is associated with transition metals, particularly copper and iron. In the absence of these ions, hydrogen peroxide remains relatively stable. Disruption of the homeostasis of these metals leads to the formation of hydroxyl radicals through the Fenton reaction. Hydroxyl radicals are

acknowledged as the most reactive ROS, capable of interacting with virtually any biomolecule (*e.g.*, proteins, DNA), resulting in the formation of toxic compounds and subsequently causing cellular damage (Damasceno *et al*. 2020). The experiments revealed that all fermentation samples exhibited substantial metal chelating ability, particularly in relation to copper, as well as hydroxyl radical scavenging capability. Given that the numerical value of hydroxyl radical scavenging activity significantly surpasses that of metal chelating activity, it was hypothesized that fermentation sample could prevent ROS formation and cascade reactions at the initiation phase of oxidation *via* multiple mechanisms, including the removal of metal ions. Moreover, fermentation samples showed strong free radical scavenging activity, with DPPH and superoxide scavenging rates of 60.24% and 40.55% in ASF, 64.20% and 49.42% in CF, as well as 69.48% and 61.32% in AEC, respectively, which demonstrated their broad ROS scavenging capacity. In addition, AEC exhibited the highest antioxidant capacity, with a FRAP value of 1.36 mmol eq. $FeSO_4$/mL, followed by the CF. The highest antioxidant ability of AEC may be attributed to its highest content of phenolics, such as tannins and anthocyanins. These findings demonstrated that all the samples are excellent multitarget antioxidants with great potential for protection against UV-induced OS by inhibiting free radicals and acting on the initial stage of cellular compound oxidation.

Table 3. *In Vitro* Antioxidant Activity Tests of Fermentation Samples

Item (unit)	ASF	CF	AEC
FRAP (mmoL eq $FeSO_4$/mL)	0.78 ± 0.02 ^{c}	1.15 ± 0.04 ^{b}	1.36 ± 0.03 ^{a}
DPPH scavenging (%)	60.24 ± 1.02 ^{c}	64.20 ± 0.85 ^{b}	69.48 ± 0.69 ^{a}
Hydroxyl scavenging (%)	70.93 ± 2.66 ^{b}	74.14 ± 1.45 ^{b}	88.42 ± 1.05 ^{a}
Superoxide scavenging (%)	40.55 ± 0.95 ^{c}	49.42 ± 1.84 ^{b}	61.32 ± 2.58 ^{a}
Copper chelation (%)	40.73 ± 0.33 ^{c}	46.64 ± 0.47 ^{b}	66.53 ± 0.96 ^{a}
Iron chelation (%)	34.55 ± 1.35 ^{b}	33.21 ± 0.44 ^{b}	42.62 ± 3.31^{a}

FRAP: Ferrous reducing antioxidant power; DPPH: 1,1-diphenyl-2-picrylhydrazyl
Different small letters within the same item are significantly different ($p < 0.05$).

In vitro Studies

Inhibition of UV-induced death of human keratinocytes by MSFF

The viability of human keratinocytes was assessed using the SRB method. Fermentation samples were applied to HaCaT cells at three varying concentrations (0.1%, 0.5%, and 1%). As depicted in Fig. 2A, the viability of HaCaT cells exposed to these concentrations was similar to that of the control group, validating the absence of cytotoxic effects on HaCaT cells (with over 80% cell survival). Therefore, these nine fermentation sample concentrations were considered noncytotoxic and were utilized in subsequent experiments.

The HaCaT cells were pretreated with various fermentation samples at different dosages prior to exposure to 15 mJ/cm^2 of UVB radiation to evaluate their respective capacities for protecting against UV-induced apoptosis (Fig. 2B). Compared with non-exposure, UVB exposure significantly reduced the viability of HaCaT cells in the absence of fermentation sample treatment (Control group), resulting in a viability of 55.4%. Cells pretreated with the ASF sample exhibited significantly higher viability in comparison to cells treated with equivalent doses of CF and AEC samples. Moreover, the increase in HaCaT cell viability was found to be dose-dependent. The highest viability of UVB-irradiated HaCaT cells reaching 90.4%, was achieved through pretreatment with a 1.0%

ASF sample. Conversely, the AEC sample group exhibited the lowest cell viability, suggesting that fermentation products induced by acid stress in *Monascus*, such as SCFAs, possess a more potent anti-apoptotic effect. Therefore, these results indicate that acid stress enhances the ability of fermentation samples to inhibit UVB-induced apoptosis in human keratinocytes.

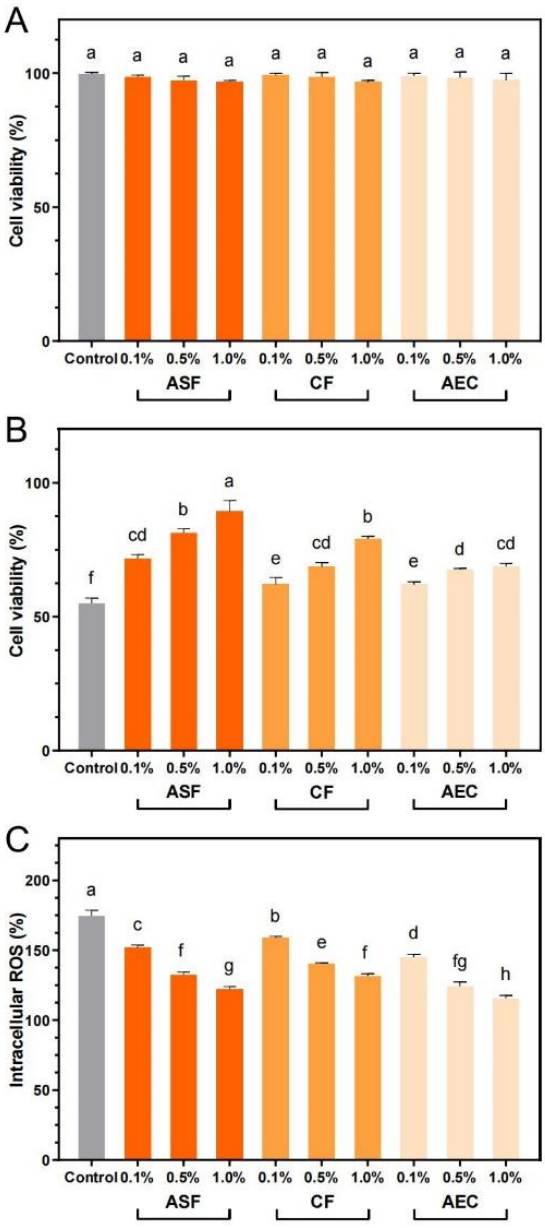

Fig. 2. *In vitro* assessment of various types and dosages of fermentation samples on cytotoxicity (A), UV-induced apoptosis (B) and UV-induced intracellular ROS production (C) in human keratinocytes. Different small letters above columns are significantly different ($p < 0.05$).

ROS-scavenging effect of the fermentation sample on UV-irradiated human keratinocytes

In light of the fact that UVB radiation induces excessive production of ROS, leading to inflammation and photoaging, the effect of various fermentation samples on the generation of UVB-induced intracellular ROS in HaCaT cells was investigated. The DCF-DA fluorescent probe was used to measure intracellular ROS levels. As shown in Fig. 2C, the fluorescence intensity in UVB-irradiated cells (Control) was significantly higher

compared to non-UVB-irradiated cells (174.5%). Conversely, pretreatment of cells with fermentation samples led to a significant reduction in UVB-induced intracellular ROS levels. The extent of this effect was contingent upon the sample concentration. ROS levels in cells treated with 1% AEC were found to be at their lowest level compared to cells pretreated with other concentrations of the sample. By contrast, cells pretreated with the ASF sample exhibited lower ROS level in comparison to cells treated with equivalent doses of CF samples. These results underscore the capacity of all the fermentation samples to effectively inhibit UVB-induced ROS production in human skin cells, corroborating previous findings indicating their robust ROS scavenging capabilities.

Anti-inflammatory effect of fermentation samples on UV-irradiated human keratinocytes

To assess the potential inhibitory effects of fermentation samples on UV-induced proinflammatory mediators, the expression levels of proinflammatory cytokines, such as IL-6 and IL-8, were examined. Overall, UV irradiation was found to elevate the expression of these proinflammatory cytokines, known to trigger inflammation and photoaging (Figs. 3A and B). Comparatively, when all fermentation samples were introduced to HaCaT cells, a significant dose-dependent reduction in UV-induced IL-6 and IL-8 expression was observed in contrast to the negative control. Remarkably, cells pre-treated with ASF demonstrated lower levels of proinflammatory cytokines at equivalent dosage levels compared to those pretreated with CF and AEC, particularly at higher concentrations. Notably, treatment with 1.0% ASF resulted in an impressive 85.2% inhibition rate of UV-mediated IL-6. These results indicate that acid stress enhances the capacity of fermentation samples to mitigate UVB-induced inflammation in human keratinocytes by reducing the levels of proinflammatory cytokines.

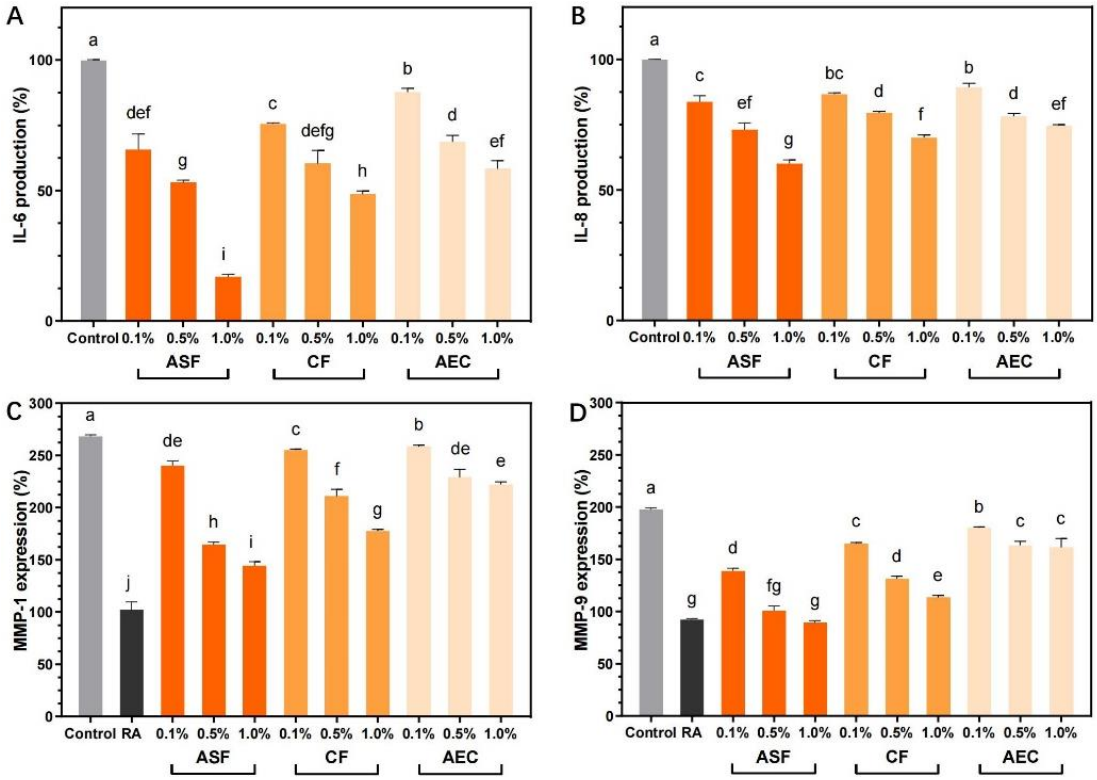

Fig. 3. *In vitro* assessment of various types and dosages of fermentation samples on IL-6 (A), IL-8 (B), MMP-1 (C), and MMP-9 (D) level in UVB-irradiated human keratinocytes. Different small letters above columns are significantly different ($p < 0.05$).

Anti-photoaging effect of MSFF on UV-irradiated human keratinocytes

The anti-photoaging effects of various fermentation samples administered at different dosages were compared in relation to a 10 µM retinoic acid (RA) standard. The evaluation focused on the ability of these samples to mitigate UV-induced expression of MMP-1 and MMP-9. All experimental groups were treated with 5 J/cm^2 of UV radiation, except for the control group. The resulting MMP expression levels are depicted in Figs. 3C and 3D.

Upon UV irradiation, MMP-1 expression levels significantly increased to 267.2%. However, treatment with fermentation samples and RA demonstrated a significant decrease in MMP-1 expression. Compared with those in UV-induced cells, MMP-1 expression levels in cells treated with 1% ASF and RA decreased to 147.8% and 107.0%, respectively. Overall, as the sample concentration increased, MMP-1 expression exhibited a decreasing trend. MMP-1 expression levels in the ASF treatment groups were significantly higher than those in the CF and AEC groups. Following UV irradiation, MMP-9 expression levels significantly increased to 197.5%. However, subsequent treatment with ASF, CF, AEC, and RA led to a marked decrease in MMP-9 expression. Notably, the MMP-9 expression level in RA-treated cells after UV irradiation did not significantly differ from that observed in cells treated with ASF concentrations exceeding 0.5%. These findings suggest that acid stress effectively enhances the anti-photoaging potential of fermentation samples by inhibiting the UV-induced expression of MMPs associated with photoaging formation.

In vivo Studies

To compare the *in vivo* anti-inflammatory and anti-photoaging effects of fermentation samples, the impact of CF and ASF on PW, pigmentation, redness, and TI was evaluated. A total of 36 healthy participants were enrolled in a 6-week study, all of them were required to spend an average of ≥6 h outdoor daily owing to their occupational obligations.

First, CF and ASF samples were compared with that of a placebo on PW using the Antera3D system (Fig. 4A). Following a 6-week treatment period, a significant reduction in PW was observed for both CF and ASF samples compared to the initial PW values. The ASF sample exhibited a higher rate of reduction (10.14%) compared to the CF sample (6.24%). In contrast, there was no statistically significant difference observed between the initial and final periorbital wrinkle values in the placebo group. Subsequently, the effects of two different samples were compared, along with a placebo, on pigmentation using the Antera3D system (Fig. 4B). After 6 weeks of treatment, there was a slight decrease in skin melanin values for the CF and ASF groups compared to their initial levels; however, these differences did not reach statistical significance. Remarkably, the placebo group experienced an increase in melanin levels compared to their initial levels. This suggests that both ASF and CF treatments have a moderate mitigating effect on UV-induced melanin overexpression.

Compared to the initial skin redness values, a decrease in redness was observed in both the CF and ASF treatment groups, as well as the placebo-treated group (Fig. 4C). However, the CF- and ASF-treated group demonstrated a substantially greater reduction in redness compared to the placebo-treated group. Moreover, the rate of decrease was significantly higher in the ASF group than in the CF group (9.78% vs. 5.06%). Furthermore, an assessment of ASF and CF in improving photoaging-induced skin

roughness was conducted. After 6 weeks of treatment, both the CF- and ASF-treated groups demonstrated a reduction in TI by 11.0% and 3.5%, respectively (Fig. 4D). Remarkably, some ASF-treated volunteers demonstrated a reduction in TI of over 20%. Overall, in line with *in vitro* findings, acid stress significantly enhanced the ability of fermented samples to mitigate various manifestations of skin inflammation and photoaging.

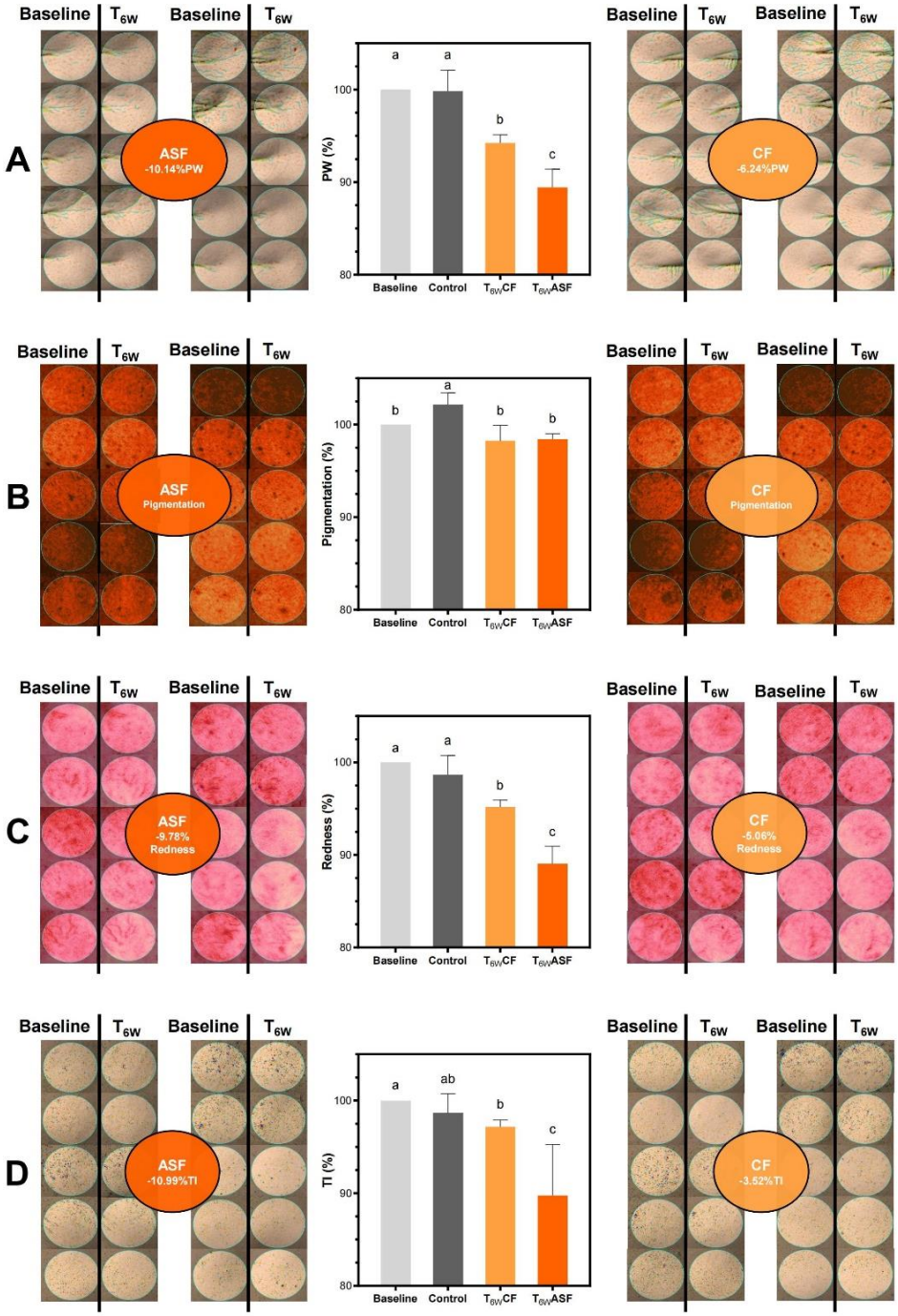

Fig. 4. Antera3D images obtained at baseline and after 6 weeks to evaluate the efficacy of CF and ASF in anti-inflammatory and anti-photoaging effect. (A) periorbital wrinkle, (B) pigmentation, (C) redness, and (D) texture index. T6W = images taken after 6 weeks of daily MSFF use; PW = Periorbital Wrinkle; TI = Texture index.

DISCUSSION

Skin aging results from complex biological mechanisms encompassing both internal factors and external stressors. Intrinsic aging represents an inexorable physiological process driven by genetic factors. Conversely, extrinsic aging is induced by external environmental stressors such as temperature fluctuations, pollution, and UV radiation (Makrantonaki and Zouboulis 2007). UV radiation-induced skin aging, referred to as photoaging, manifests as deepening wrinkles, hyperpigmentation, an uneven skin texture, and skin redness (Kovacs *et al*. 2009). It is widely acknowledged that photoaging is closely associated with OS induced by UV radiation. Prolonged direct exposure to UV leads to excessive ROS production in the epidermis, including superoxide anions, hydrogen peroxide, singlet oxygen, and hydroxyl radicals. These ROS disrupt the skin's antioxidant defense mechanisms, ultimately leading to OS. The resulting OS, in turn, triggers the production of melanin, MMPs, and proinflammatory cytokines, culminating in the visible signs of photoaging and inflammation, including pigmentation, skin wrinkling, and roughness (Pillai *et al*. 2005).

Studying novel cosmetic raw materials to alleviate skin issues arising from environmental stress, particularly photoaging, has been a prominent pursuit. Postbiotics, known for their mildness, safety, and high efficacy, have found extensive utilization in skincare (Sanders *et al*. 2019). This study investigated a novel ASF process involving *M. pilosus* YX-1125, an extremophile known for its resilience to various environmental stresses within the extreme brewing environment of a Chinese liquor (Zheng *et al*. 2021). The objective was to explore its potential for safeguarding the skin against UV-induced inflammation and photoaging. The ASF sample reduced apoptosis, redox imbalance, the production of proinflammatory cytokines, and the expression of MMP associated with the development of inflammation and photoaging. *In vivo* experiments validated that ASF exhibited superior protective effects compared to CF by ameliorating the visible signs of inflammation and photoaging, such as hyperpigmentation, skin redness, facial wrinkles, and periorbital fine lines. This study marks the first demonstration of the applicability of extremophile-derived ASF products in skincare, offering protection against damage induced by environmental stressors.

UV exposure results in the manifestation of photoaging signs in the skin, such as a rough, dry texture, and intensified wrinkles. UV-induced OS can induce the expression of MMPs by activating various signaling pathways, including MAPKs and nuclear factor-κB. MMPs play a pivotal role in the degradation of extracellular matrix (ECM) proteins such as collagen, fibronectin, elastin, and proteoglycans, ultimately contributing to the process of photoaging (Pittayapruek *et al*. 2016). Among MMPs, MMP-1 (collagenase) and MMP-9 (gelatinase) are responsible for degrading the majority of the ECM in the skin. Their overexpression stands as the leading cause of photoaging-related wrinkle formation (Lu *et al*. 2011). In this study, exposure to UV irradiation significantly increased the expression of MMP-1 and MMP-9 in HaCaT cells; however, this upregulation was significantly mitigated following treatment with ASF and RA. Moreover, volunteers treated with ASF displayed an improvement in facial texture and periorbital fine lines. These findings suggest that ASF samples effectively hinder UV-induced skin photoaging by inhibiting MMP expression. Several previous studies have attempted to prevent skin photoaging by inhibiting MMP expression. Lin *et al*. (2022) demonstrated the potential of *Pholiota nameko* polysaccharides (PNPs) in ameliorating photoaging. The application of PNPs resulted in a reduction of MMP-1, MMP-3, and MMP-9 expression in human hypodermal

cells and significantly alleviated UVA-induced cellular senescence. In another study, Karapetsas *et al.* (2020) investigated the effect of Greek honey extract on UVB-treated HaCaT cells. They showed a significant augmentation of MMP expression with the honey extract, leading to antiaging effects and photoprotection, which were further validated in a reconstituted skin model.

In the context of UV-induced OS, redox homeostasis disruption within skin cells leads to cellular damage, culminating in inflammation and apoptosis. Extensive evidence supports the notion that UV irradiation-triggered apoptosis in skin cells results from the synergistic interplay between mitochondrial (intrinsic) and death receptor (extrinsic) pathways (Lee *et al*. 2013). Moreover, chronic UV exposure amplifies the production of proinflammatory mediators such as IL-1α, IL-1β, IL-6, IL-8, prostaglandin E2, and nitric oxide (Yoshizumi *et al*. 2008). Wang *et al*. (2022) investigated the effect of Prinsepiae Nux extract on UVB-induced inflammation in HaCaT cells. They found that UVB-induced deficiencies in nuclear factor erythroid 2–related factor 2 and heme oxygenase-1, along with excessive ROS production and upregulation of proinflammatory mediator genes, were variably reversed. Consequently, this extract effectively safeguarded skin cells from UV-induced damage (Wang *et al*. 2022). Charachit *et al.* (2022) examined the potential mechanisms of *Houttuynia cordata* extract against UV-induced apoptosis and inflammation in HaCaT cells. They found that the extract of *H. cordata* along with its active compounds, significantly diminished the UVB-induced expression of proinflammatory cytokines, including IL-6, IL-8, cyclooxygenase-2, and inducible nitric oxide synthase. Additionally, it activated caspase-9 and caspase-3 to prevent UVB irradiation-induced apoptosis inhibition in HaCaT cells. Furthermore, it regulated the MAPK and Akt signaling pathways, effectively protecting HaCaT cells against UVB-induced oxidative damage and inflammation (Charachit *et al*. 2022). In the present study, ASF effectively reduced UVB-induced apoptosis in HaCaT cells and decreased the expression of proinflammatory cytokines, such as IL-6 and IL-8, in a dose-dependent manner. *In vivo* experiments corroborated the findings of *in vitro* experiments. After 6 weeks of ASF use, study participants demonstrated a significant reduction in facial redness. Notably, a 1% ASF sample inhibited over 80% of UVB-induced proinflammatory cytokines, a considerably higher efficacy than reported in the aforementioned literature. This underscores the exceptional anti-inflammatory potential of ASF, which may be attributed to its rich content of bioactive compounds such as SCFAs and phenolics.

Extremophiles are microorganisms capable of thriving in the harshest ecological niches. Over extended periods of extreme environmental stress, they have developed unique genotypes and phenotypes distinct from those of typical microorganisms, as a means to manage intracellular OS induced by the harsh external conditions (Kruger *et al*. 2018). Due to their remarkable phenotypic and genotypic adaptability, extremophiles represent a promising avenue for biotechnological applications. They can adapt to unfavorable environments and produce efficient metabolites, enzymes, and cells even under extreme conditions (Giovanella *et al*. 2020). In this context, the extremophile strain YX-1125, which exhibits tolerance to acidic conditions, was isolated from the extreme brewing environment of Moutai Town, China. In an unprecedented study, the fermentation product of this strain, subjected to acid stress, was applied to assess its potential in protecting the skin from UV-induced inflammation and photoaging. A previous study showed that YX-1125 primarily produces SCFAs as metabolites under extreme environmental stress conditions, resulting in elevated SCFAs levels.

Most SCFAs, particularly acetic acid, propionic acid, and butyric acid, are predominantly found in probiotic fermentation products in the gut. They exert a myriad of effects on human physiology, serving as a cellular energy source (Kaiko *et al*. 2016), regulating and repairing physiological barriers (Kelly *et al*. 2015), and influencing inflammatory responses (Koh *et al*. 2016). Wang *et al*. (2014) demonstrated the effective suppression of skin inflammation and the growth of *Cutibacterium acnes* and *Pseudomonas* by SCFAs. Similarly, in the present study, elevated levels of SCFAs were detected in the ASF sample, likely contributing to its robust anti-inflammatory and cytoprotective properties.

Phenolic compounds constitute another active substance found in ASF, occurring in significant concentrations. The antioxidant properties of plant-derived phenolic compounds have been extensively documented in several studies (Cadiz-Gurrea *et al*. 2021). Phenolic compounds are secondary metabolites in plants known for their exceptional antioxidant capabilities and UV-blocking attributes, thereby offering significant benefits for skin care and the mitigation of skin aging by alleviating OS damage (Rodrigues *et al*. 2015). Innovative skincare formulations enriched with phenolic compounds have gained widespread use in commercially available cosmetic products due to their robust antioxidant and antimicrobial properties, as well as their ability to protect against UV-induced damage, and inhibit MMPs. Hong *et al*. (2020) demonstrated the abundant presence of potent antioxidant and anti-inflammatory phenolic compounds in sorghum. In the present study, there was a high concentration of phenolic compounds in ASF, which may have been released during the fermentation process of sorghum. The combination of SCFAs and phenolic compounds, both abundant in ASF, may account for its capacity to mitigate skin damage associated with inflammation and photoaging.

CONCLUSIONS

1. *In vitro* and *in vivo* experiments demonstrated that exposure to acid stress enhances the UV-induced skin damage protection capability of a fermentation sample derived from an extremophile strain.
2. Acid-stress fermentation (ASF) of sorghum by *M. pilosus* provided a fermentation product under acid stress. It was found to be rich in short-chain fatty acids (SCFAs) and phenolic compounds, exhibiting robust and multifaceted antioxidant properties that effectively mitigate various adverse effects caused by UV irradiation on the skin. These effects include inflammation, oxidative stress (OS), wrinkle formation, and pigmentation.
3. Collectively, the data support the conclusion that ASF outperformed conventional fermentation (CF) as a skin care product in terms of its anti-inflammatory and anti-photoaging properties. This highlights its potential to serve as a valuable ingredient in functional cosmetics.
4. In addition, this is the first study to demonstrate the utility of extremophile fermentation products in safeguarding the skin against environmental stressors.

ACKNOWLEDGMENTS

This research was funded by the National Natural Science Foundation of China [grant number, 52160006], the Research Foundation for Scientific Scholars of Moutai Institute, the Scientific Research Foundation of Southwest Medical University [grant number, 2021ZKZD011] and the joint foundation of Luzhou government and Southwest Medical University [grant number, 2021LZXNYD-D08].

Data Availability Statement

The data that support the findings of this study are available from the corresponding author [J.F.], upon reasonable request.

Author Contributions

Yuxi Zheng and Han Luo contributed equally in this study performing the experiments and preparing the first draft of the manuscript; Nianhui Ding, Yan Huang, Kai Wang, Chun Li and Chaolong Zhang contributed to the acquisition and analysis of data; Yuxi Zheng, Kai Wang, and Jianguo Feng acquired the founding; Jianguo Feng design of the work, supervised and finalized the manuscript. All authors read and approved the final manuscript.

Informed Consent Statement

Written informed consent was obtained from all participants involved in the study.

Conflict of Interest Disclosure

The authors declare no conflict of interest.

REFERENCES CITED

Adebo, O. A. (2020). "African sorghum-based fermented foods: Past, current and future prospects, " *Nutrients* 12, article 1111. DOI: 10.3390/nu12041111

Cadiz-Gurrea, M. L., Pinto, D., Delerue-Matos, C., and Rodrigues, F. (2021). "Olive fruit and leaf wastes as bioactive ingredients for cosmetics-A preliminary study," *Antioxidants (Basel)* 10(2), article 245. DOI: 10.3390/antiox10020245

Carlson, R. V., Boyd, K. M., and Webb, D. J. (2004). "The revision of the Declaration of Helsinki: past, present and future," *Br. J. Clin. Pharmacol.* 57, 695-713. DOI: 10.1111/j.1365-2125.2004.02103.x

Charachit, N., Sukhamwang, A., Dejkriengkraikul, P., and Yodkeeree, S. (2022). "Hyperoside and quercitrin in *Houttuynia cordata* extract attenuate UVB-induced human keratinocyte cell damage and oxidative stress *via* modulation of MAPKs and Akt signaling pathway," *Antioxidants (Basel)* 11(2), article 221. DOI: 10.3390/antiox11020221

Chen, G. Q., and Jiang, X. R. (2018). "Next generation industrial biotechnology based on extremophilic bacteria," *Curr. Opin. Biotechnol.* 50, 94-100. DOI: 10.1016/j.copbio.2017.11.016

Dai, Y., Tian, Z., Meng, W., and Li, Z. (2020). "Microbial diversity and physicochemical characteristics of the maotai-flavored liquor fermentation process," *J. Nanosci. Nanotechnol.* 20, 4097-4109. DOI: 10.1166/jnn.2020.17522

Damasceno, G. A. B., Barreto, S., Reginaldo, F. P. S., Souto, A. L., Negreiros, M. M. F., Viana, R. L. S., Pinto, T. K. B., Daher, C. C., Silva-Filho, J. A. A., Moura, R. A. O., Silva, M. A., Silveira, W. L. L., Medeiros, A. A., Ostrosky, E. A., Verissimo, L. M., Sassaki, G. L., Lopes, P. S., Sales, V. S. F., Rocha, H. A. O., Cavalheiro, A. J., Giordani, R. B., and Ferrari, M. (2020). "*Prosopis juliflora* as a new cosmetic ingredient: Development and clinical evaluation of a bioactive moisturizing and anti-aging innovative solid core," *Carbohydr. Polym.* 233, article 115854. DOI: 10.1016/j.carbpol.2020.115854

Dia, V. P., Pangloli, P., Jones, L., McClure, A., and Patel, A. (2016). "Phytochemical concentrations and biological activities of Sorghum bicolor alcoholic extracts," *Food Funct.* 7, 3410-3420. DOI: 10.1039/c6fo00757k

Fitsiou, E., Pulido, T., Campisi, J., Alimirah, F., and Demaria, M. (2021). "Cellular senescence and the senescence-associated secretory phenotype as drivers of skin photoaging," *J. Invest. Dermatol.* 141, 1119-1126. DOI: 10.1016/j.jid.2020.09.031

Galati, A., Oguntoyinbo, F. A., Moschetti, G., Crescimanno, M., and Settanni, L. (2014). "The cereal market and the role of fermentation in cereal-based food production in Africa," *Food Rev. Int.* 30, 317-337. DOI: 10.1080/87559129.2014.929143

Giovanella, P., Vieira, G. A. L., Ramos Otero, I. V., Pais Pellizzer, E., de Jesus Fontes, B., and Sette, L. D. (2020). "Metal and organic pollutants bioremediation by extremophile microorganisms," *J. Hazard. Mater.* 382, article 121024. DOI: 10.1016/j.jhazmat.2019.121024

Gu, Y., Han, J., Jiang, C., and Zhang, Y. (2020). "Biomarkers, oxidative stress and autophagy in skin aging," *Ageing Res. Rev.* 59, article 101036. DOI: 10.1016/j.arr.2020.101036

Hong, S., Pangloli, P., Perumal, R., Cox, S., Noronha, L. E., Dia, V. P., and Smolensky, D. (2020). "A comparative study on phenolic content, antioxidant activity and anti-inflammatory capacity of aqueous and ethanolic extracts of sorghum in lipopolysaccharide-induced RAW 264.7 macrophages," *Antioxidants (Basel)* 9. DOI: 10.3390/antiox9121297

Huang, J. L., Wang, H. H., Alam, F., and Cui, Y. W. (2019). "Granulation of halophilic sludge inoculated with estuarine sediments for saline wastewater treatment," *Sci. Total Environ.* 682, 532-540. DOI: 10.1016/j.scitotenv.2019.05.197

Kaiko, G. E., Ryu, S. H., Koues, O. I., Collins, P. L., Solnica-Krezel, L., Pearce, E. J., Pearce, E. L., Oltz, E. M., and Stappenbeck, T. S. (2016). "The colonic crypt protects stem cells from microbiota-derived metabolites," *Cell* 167, article 1137. DOI: 10.1016/j.cell.2016.10.034

Karapetsas, A., Voulgaridou, G. P., Iliadi, D., Tsochantaridis, I., Michail, P., Kynigopoulos, S., Lambropoulou, M., Stavropoulou, M. I., Stathopoulou, K., Karabournioti, S., Aligiannis, N., Gardikis, K., Galanis, A., Panayiotidis, M. I., and Pappa, A. (2020). "Honey extracts exhibit cytoprotective properties against UVB-induced photodamage in human experimental skin models," *Antioxidants (Basel)* 9. DOI: 10.3390/antiox9070566

Kelly, C. J., Zheng, L., Campbell, E. L., Saeedi, B., Scholz, C. C., Bayless, A. J., Wilson, K. E., Glover, L. E., Kominsky, D. J., Magnuson, A., Weir, T. L., Ehrentraut, S. F., Pickel, C., Kuhn, K. A., Lanis, J. M., Nguyen, V., Taylor, C. T., and Colgan, S. P. (2015). "Crosstalk between microbiota-derived short-chain fatty acids and intestinal epithelial HIF augments tissue barrier function," *Cell Host Microbe* 17, 662-671. DOI: 10.1016/j.chom.2015.03.005

Koh, A., De Vadder, F., Kovatcheva-Datchary, P., and Backhed, F. (2016). "From dietary fiber to host physiology: Short-chain fatty acids as key bacterial metabolites," *Cell* 165, 1332-1345. DOI: 10.1016/j.cell.2016.05.041

Kovacs, D., Raffa, S., Flori, E., Aspite, N., Briganti, S., Cardinali, G., Torrisi, M. R., and Picardo, M. (2009). "Keratinocyte growth factor down-regulates intracellular ROS production induced by UVB," *J. Dermatol. Sci.* 54, 106-113. DOI: 10.1016/j.jdermsci.2009.01.005

Kruger, A., Schafers, C., Schroder, C., and Antranikian, G. (2018). "Towards a sustainable biobased industry - Highlighting the impact of extremophiles," *N. Biotechnol.* 40, 144-153. DOI: 10.1016/j.nbt.2017.05.002

Lee, C. H., Wu, S. B., Hong, C. H., Yu, H. S., and Wei, Y. H. (2013). "Molecular mechanisms of UV-induced apoptosis and its effects on skin residential cells: The implication in UV-based phototherapy," *Int. J. Mol. Sci.* 14, 6414-6435. DOI: 10.3390/ijms14036414

Lin, H., Cheng, K. C., Lin, J. A., Hsieh, L. P., Chou, C. H., Wang, Y. Y., Lai, P. S., Chu, P. C., and Hsieh, C. W. (2022). "*Pholiota nameko* polysaccharides protect against ultraviolet A-induced photoaging by regulating matrix metalloproteinases in human dermal fibroblasts," *Antioxidants (Basel)* 11(4), article 739. DOI: 10.3390/antiox11040739

Liu, Y., Liu, J., Dai, H., Wang, R., Hsiao, A., Wang, W., Betts, R. J., Marionnet, C., Bernerd, F., and Qiu, J. (2022). "Photo-aging evaluation - In vitro biological endpoints combined with collagen density assessment with multi-photon microscopy," *J. Dermatol. Sci.* 105, 37-44. DOI: 10.1016/j.jdermsci.2021.12.002

Lloyd-Price, J., Arze, C., Ananthakrishnan, A. N., Schirmer, M., Avila-Pacheco, J., Poon, T. W., Andrews, E., Ajami, N. J., Bonham, K. S., Brislawn, C. J., Casero, D., Courtney, H., Gonzalez, A., Graeber, T. G., Hall, A. B., Lake, K., Landers, C. J., Mallick, H., Plichta, D. R., Prasad, M., Rahnavard, G., Sauk, J., Shungin, D., Vazquez-Baeza, Y., White, R. A., 3rd, Investigators, I., Braun, J., Denson, L. A., Jansson, J. K., Knight, R., Kugathasan, S., McGovern, D. P. B., Petrosino, J. F., Stappenbeck, T. S., Winter, H. S., Clish, C. B., Franzosa, E. A., Vlamakis, H., Xavier, R. J., and Huttenhower, C. (2019). "Multi-omics of the gut microbial ecosystem in inflammatory bowel diseases," *Nature* 569, 655-662. DOI: 10.1038/s41586-019-1237-9

Lu, P., Takai, K., Weaver, V. M., and Werb, Z. (2011). "Extracellular matrix degradation and remodeling in development and disease," *Cold Spring Harb. Perspect. Biol.* 3(12), article a005058. DOI: 10.1101/cshperspect.a005058

Maitriwong, P., Tangkijngamvong, N., and Asawanonda, P. (2020). "Innovative 1064-nm Nd:YAG laser significantly improves keratosis pilaris, A randomized, double-blind, sham-irradiation-controlled trial," *Lasers Surg. Med.* 52, 509-514. DOI: 10.1002/lsm.23184

Makrantonaki, E., and Zouboulis, C. C. (2007). "Molecular mechanisms of skin aging: State of the art," *Ann. N Y Acad. Sci.* 1119, 40-50. DOI: 10.1196/annals.1404.027

Mellinas, C., Solaberrieta, I., Pelegrin, C. J., Jimenez, A., and Garrigos, M. C. (2022). "Valorization of agro-industrial wastes by ultrasound-assisted extraction as a source of proteins, antioxidants and cutin: A cascade approach," *Antioxidants (Basel)* 11(9), article 1739. DOI: 10.3390/antiox11091739

Olsen, J., Gaetti, G., Grandahl, K., and Jemec, G. B. E. (2022). "Optical coherence tomography quantifying photo aging: skin microvasculature depth, epidermal thickness and UV exposure," *Arch. Dermatol. Res.* 314, 469-476. DOI: 10.1007/s00403-021-02245-8

Orellana, E. A., and Kasinski, A. L. (2016). "Sulforhodamine B (SRB) assay in cell culture to investigate cell proliferation," *Bio. Protoc.* 6(21), article e1984. DOI: 10.21769/BioProtoc.1984

Osman, A., El-Wahab, A. A., Ahmed, M. F. E., Buschmann, M., Visscher, C., Hartung, C. B., and Lingens, J. B. (2022). "Nutrient composition and in vitro fermentation characteristics of sorghum depending on variety and year of cultivation in northern Italy, " *Foods (Basel, Switzerland)* 11, article 3255. DOI:10.3390/foods11203255

Peng, L., Kong, X., Wang, Z., Ai-Lati, A., Ji, Z., and Mao, J. (2021). "Baijiu vinasse as a new source of bioactive peptides with antioxidant and anti-inflammatory activity," *Food Chem* 339, article 128159. DOI: 10.1016/j.foodchem.2020.128159

Pillai, S., Oresajo, C., and Hayward, J. (2005). "Ultraviolet radiation and skin aging: roles of reactive oxygen species, inflammation and protease activation, and strategies for prevention of inflammation-induced matrix degradation - a review," *Int. J. Cosmet. Sci.* 27, 17-34. DOI: 10.1111/j.1467-2494.2004.00241.x

Pittayapruek, P., Meephansan, J., Prapapan, O., Komine, M., and Ohtsuki, M. (2016). "Role of matrix metalloproteinases in photoaging and photocarcinogenesis," *Int. J. Mol. Sci.* 17(6), article 868. DOI: 10.3390/ijms17060868

Rerknimitr, P., Tekacharin, N., Panchaprateep, R., Wititsuwannakul, J., Tangtanatakul, P., Hirankarn, N., and Asawanonda, P. (2019). "Pulsed-dye laser as an adjuvant treatment for discoid lupus erythematosus: a randomized, controlled trial," *J. Dermatolog. Treat.* 30, 81-86. DOI: 10.1080/09546634.2018.1468063

Rittie, L., and Fisher, G. J. (2015). "Natural and sun-induced aging of human skin," *Cold Spring Harb. Perspect. Med.* 5, article a015370. DOI: 10.1101/cshperspect.a015370

Rodrigues, F., Pimentel, F. B., and Oliveira, M. B. P. P. (2015). "Olive by-products: Challenge application in cosmetic industry," *Industrial Crops and Products* 70, 116-124. DOI: 10.1016/j.indcrop.2015.03.027

Sanders, M. E., Merenstein, D. J., Reid, G., Gibson, G. R., and Rastall, R. A. (2019). "Probiotics and prebiotics in intestinal health and disease: From biology to the clinic," *Nat. Rev. Gastroenterol. Hepatol.* 16, 605-616. DOI: 10.1038/s41575-019-0173-3

Schuch, A. P., Moreno, N. C., Schuch, N. J., Menck, C. F. M., and Garcia, C. C. M. (2017). "Sunlight damage to cellular DNA: Focus on oxidatively generated lesions," *Free Radic. Biol. Med.* 107, 110-124. DOI: 10.1016/j.freeradbiomed.2017.01.029

Shahab, R. L., Brethauer, S., Davey, M. P., Smith, A. G., Vignolini, S., Luterbacher, J. S., and Studer, M. H. (2020). "A heterogeneous microbial consortium producing short-chain fatty acids from lignocellulose," *Science* 369(6507), article eabb1214. DOI: 10.1126/science.abb1214

Shen, S., Huang, R., Li, C., Wu, W., Chen, H., Shi, J., Chen, S., and Ye, X. (2018). "Phenolic compositions and antioxidant activities differ significantly among sorghum grains with different applications," *Molecules* 23. DOI: 10.3390/molecules23051203

Sun, H., Wang, H., Zhang, P., Ajlouni, S., and Fang, Z. (2020). "Changes in phenolic content, antioxidant activity, and volatile compounds during processing of fermented sorghum grain tea," *Cereal Chem.* 97, 612-625. DOI: 10.1002/cche.10277

Tanwar, R., Panghal, A., Chaudhary, G., Kumari, A., and Chhikara, L.(2023). "Nutritional, phytochemical and functional potential of sorghum: A review," *Food Chem. Adv.* 3, article 100501. DOI: 10.1016/j.focha.2023.100501

Wang, S. H., Chen, Y. S., Lai, K. H., Lu, C. K., Chang, H. S., Wu, H. C., Yen, F. L., Chen, L. Y., Lee, J. C., and Yen, C. H. (2022). "Prinsepiae nux extract activates NRF2 activity and protects UVB-induced damage in keratinocyte," *Antioxidants (Basel)* 11(9), article 1755. DOI: 10.3390/antiox11091755

Wang, Y., Kuo, S., Shu, M., Yu, J., Huang, S., Dai, A., Two, A., Gallo, R. L., and Huang, C. M. (2014). "*Staphylococcus epidermidis* in the human skin microbiome mediates fermentation to inhibit the growth of *Propionibacterium acnes*: Implications of probiotics in acne vulgaris," *Appl. Microbiol. Biotechnol.* 98, 411-424. DOI: 10.1007/s00253-013-5394-8

Wang, Y., Liu, H., Zhang, D., Liu, J., Wang, J., Wang, S., and Sun, B. (2019). "Baijiu vinasse extract scavenges glyoxal and inhibits the formation of N(epsilon)-carboxymethyllysine in dairy food," *Molecules* 24(8), article 1526. DOI: 10.3390/molecules24081526

Weiss, T., Zhao, J., Hu, R., Liu, M., Li, Y., Zheng, Y., Smith, G., and Wang, D. (2022). "Production of distilled spirits using grain sorghum through liquid fermentation," *J. Agric. Food Res.* 9, article 100314. DOI:10.1016/j.jafr.2022.100314

Xu, H., Hong, J. H., Kim, D., Jin, Y. H., Pawluk, A. M., and Mah, J. H. (2022). "Evaluation of bioactive compounds and antioxidative activity of fermented green tea produced *via* one- and two-step fermentation," *Antioxidants (Basel)* 11(8), article 1425. DOI: 10.3390/antiox11081425

Yoshizumi, M., Nakamura, T., Kato, M., Ishioka, T., Kozawa, K., Wakamatsu, K., and Kimura, H. (2008). "Release of cytokines/chemokines and cell death in UVB-irradiated human keratinocytes, HaCaT," *Cell Biol. Int.* 32, 1405-1411. DOI: 10.1016/j.cellbi.2008.08.011

Zheng, Y., Wang, Y., Zhang, J., and Pan, J. (2016). "Using tobacco waste extract in pre-culture medium to improve xylose utilization for l-lactic acid production from cellulosic waste by *Rhizopus oryzae*," *Bioresource Technol.* 218, 344-350. DOI: 10.1016/j.biortech.2016.06.071

Zheng, Y., Zhang, T., Lu, Y., and Wang, L. (2021). "*Monascus pilosus* YX-1125: An efficient digester for directly treating ultra-high-strength liquor wastewater and producing short-chain fatty acids under multiple-stress conditions," *Bioresource Technol.* 331, article 125050. DOI: 10.1016/j.biortech.2021.125050

Zheng, Y. X., Wang, Y. L., Pan, J., Zhang, J. R., Dai, Y., and Chen, K. Y. (2017). "Semi-continuous production of high-activity pectinases by immobilized Rhizopus oryzae using tobacco wastewater as substrate and their utilization in the hydrolysis of pectin-containing lignocellulosic biomass at high solid content," *Bioresource Technol.* 241, 1138-1144. DOI: 10.1016/j.biortech.2017.06.066

Zhou, L., Wang, C., Gao, X., Ding, Y., Cheng, B., Zhang, G., Cao, N., Xu, Y., Shao, M., and Zhang, L. (2020). "Genome-wide variations analysis of sorghum cultivar Hongyingzi for brewing Moutai liquor," *Hereditas* 157(1), article 19. DOI: 10.1186/s41065-020-00130-4

Article submitted: April 15, 2024; Peer review completed: June 1, 2024; Revised version received: June 5, 2024; Accepted: June 6, 2024; Published: June 18, 2024.
DOI: 10.15376/biores.19.3.5239-5261